



## 6<sup>th</sup> International Symposium on Solid Mechanics

Click on the box to select the Mini-Symposia:

- Multiaxial and Fretting Fatigue (*Edgar Mamiya and LucivalMalcher*);
- CompositeMaterials (*Ricardo de Medeiros*);
- Constitutive Models I – Plasticity and Damage (*LucivalMalcher, Miguel Vaz Jr. and Edgar Mamiya*);
- Constitutive Models II – Viscoelastic and Viscoplastic Solids: Models and Applications (*HeraldoMattos*);
- Impact Engineering (*Marcílio Alves*);
- Structural Reliability Methods and Reliability-Based Design Optimization (*André Beck*);
- Topology Optimization of Multifunctional Materials, Fluids and Structures (*Eduardo Lenz Cardoso e Emilio Carlos Nelli Silva*);
- Topological Derivatives: Theory and Applications (*André Novotny*);
- X-FEM, G-FEM and Meshfree Methods (*Roberto Dalledone Machado and Rodrigo Rossi*);
- High OrderFinite Elements (*Marco LúcioBittencourt*);
- Nonlinear Analyses (*Eduardo Campello*);
- Other section;

## Computational Simulations Using the Higher Order Stable Generalized Finite Element Method

**Fernando Massami Sato**

Department of Structural Engineering  
Engineering School of São Carlos, University of São Paulo  
fernandomsato@gmail.com

**Dorival Piedade Neto**

Department of Structural Engineering  
Engineering School of São Carlos, University of São Paulo  
dpiedade@sc.usp.br

**Sergio Persival Baroncini Proença**

Department of Structural Engineering  
Engineering School of São Carlos, University of São Paulo  
persival@sc.usp.br

### ABSTRACT

The Stable Generalized Finite Element Method (SGFEM) is essentially an improved version of the Generalized Finite Element Method (GFEM). Besides of retaining the good flexibility for constructing local enriched approximations, the SGFEM has the advantage of presenting much better conditioning than that of the conventional GFEM. Actually, bad conditioning is well known as one of the main drawbacks of the GFEM, while affecting severely the precision of the numerical scheme used for solving the linear system associated to the problem. Despite of its consistent mathematical basis, the numerical experiments so far conducted on using SGFEM are not yet clearly conclusive, especially regarding the robustness of the method.

Therefore, the main purpose of the present paper is to give a contribution in this direction, through further investigating the SGFEM accuracy and stability. In particular, the recent proposed version of the method, called higher order SGFEM, is hereby considered. Some computational aspects are briefly addressed, as the ones related to the implementation and integration of a flat-top partition of unit for constructing the augmented approximation space with polynomial enrichments. The computational simulations consist essentially of two-dimensional linear analysis of solids with edge cracks and reentrant corners on its boundaries.

Our findings from the numerical tests done are highly relevant regarding conditioning control and order of convergence provided by the SGFEM compared to the conventional GFEM.

**Keywords:** Generalized/Stable Finite Element Method; system conditioning; numerical stability.

### 1 INTRODUCTION

The Generalized Finite Element Method (GFEM) is a Partition of Unity (PoU) based Galerkin method, according to which the basic approximation space provided by a PoU is enlarged by the product of it by functions with good approximation skills, referred to as enrichment functions. The

key concept behind such procedure is that the product of the PoU functions with any given enrichment function can exactly reproduce it. In fact, this concept was primarily introduced in the Partition of Unity Method (PUM) framework, [1].

The GFEM and the eXtended Finite Element Method (XFEM), [2], are both PoU based methods sharing the same fundamentals. In particular, a mesh of finite elements is used to provide a PoU, which is commonly defined through the piecewise linear Lagrangian shape functions embodied in the elements. Owing to such special feature and also considering that the unity is always taken as the first component of the set of enrichment functions, the GFEM/XFEM can also be understood as an extension of the conventional Finite Element Method (FEM) for which the local approximations provided by the shape functions are enlarged by means of enrichment functions.

The GFEM/XFEM enrichment framework, while dispensing with costly mesh refinements, has proved to be efficient in a variety of applications, mainly when the solution's local behavior is of major interest and, therefore, must be properly reproduced. Problems of the Linear Fracture Mechanics are likely among the most benefited by the method. For instance, crack tip stress concentrations are better mimicked by enriching the approximation through branch functions at patches nearby the tip, as suggested for instance in [3-8]. Furthermore, mesoscale cracking modeling of polycrystalline materials, as well modeling of solids containing interfaces, voids and inclusions, see [9,10], are further classes of problems in which the GFEM/XFEM features are advantageous with respect to conventional FEM approaches.

Even though the GFEM is being successfully applied to solve a wide class of mechanical problems, an improper choice of the enrichment functions can cause bad conditioning of the global stiffness matrix, therefore affecting severely the precision of the numerical scheme used for solving the linear system associated to the discretized weak form of the problem. So, the conditioning of the GFEM could be much worse than that of the standard FEM and, ultimately, have a negative effect on the robustness of the method.

The Stable Generalized Finite Element Method (SGFEM), [11], was conceived to overcome the conditioning issue and in essence is an improved version of the GFEM. In effect, besides of retaining the good flexibility for constructing local enriched approximations, the SGFEM has the advantage of presenting much better conditioning than that of the conventional GFEM. Despite of its consistent mathematical basis, the numerical experiments so far conducted on using SGFEM are not yet clearly conclusive, especially regarding the robustness of the method. Therefore, the method still demands further practical investigation on the accuracy and stability properties compared to the standard GFEM and conventional FEM approaches. The main purpose of the present paper is to give a contribution in this direction by means of computational experiments for investigating the SGFEM accuracy and stability.

In particular, the recent proposed version of the method, called higher order SGFEM, is hereby considered, [12]. In line with this reference only shifted polynomial functions of second degree are used as enrichment of the approximation. Moreover, for constructing the enrichment part of the augmented approximation space a 'flat-top' type function is used as PoU in replacement to the usual piecewise linear hat functions, that are still preserved for the basic part of the approximation space.

Some computational aspects are briefly addressed, as the ones related to the implementation and integration of a flat-top partition of unit locally at the element level. The model problems considered in the computational experiments consist of two-dimensional linear analysis of panels

presenting edge cracks and reentrant corners. Actually, these problems are typically useful to demonstrate the efficacy of the GFEM for exploring special enrichments. However, as already mentioned only polynomial enrichments are considered, since the good conditioning provided by the SGFEM is the main concern hereby emphasized.

Our findings from the computational tests done are highly relevant while confirming the favorable features of good conditioning and order of convergence, which can be proved analytically once certain assumptions on the augmented approximation space are satisfied. In particular, the resulting scaled condition numbers, similar to the ones exhibited by the conventional FEM, indicate the advantage of the higher order SGFEM compared to the standard GFEM regarding to the issue of numerical stability.

The remaining of the paper is organized in the following way. In Section 2, the weak form of the Boundary Value Problem is addressed followed by an introduction on the GFEM and SGFEM main features. In section 3 the higher order SGFEM is described. Next, some computational aspects are concisely emphasized, as the ones related to the implementation and integration of a flat-top partition of unit for constructing the augmented approximation space with polynomial enrichments. In section 4, the results of computational experiments on problems selected for analysis are shown. Finally, in Section 5, some important conclusions regarding the accuracy and numerical conditioning provided by the higher order SGFEM are emphasized.

## 2 THE WEAK FORM OF THE BOUNDARY VALUE PROBLEM (BVP)

The weak statement of the static equilibrium problem of a linear elastic solid is hereby provided in a Galerkin approach by the Principle of Virtual Work, which reads: find the small displacement field  $u \in V_t$  such that for  $\forall \delta u \in V$

$$\int_{\Omega} [\mathbb{D} \nabla^s u : \nabla^s \delta u] d\Omega = \int_{\Omega} f \delta u d\Omega + \int_{\Gamma_N} t \delta u d\Gamma \quad (1)$$

Where  $V_t$  is the standard space of trial functions for the elasticity problem and  $V$  the space of test functions, respectively defined as

$$V_t = \left\{ u \in H^1(\Omega) : u = \bar{u}(X, t) \text{ for } X \text{ on } \Gamma_D \right\} \quad (2)$$

$$V = \left\{ w \in H^1(\Omega) : w = 0 \text{ for } X \text{ on } \Gamma_D \right\} \quad (3)$$

In the relations above  $\Omega$  denotes the domain occupied by the body, with boundary  $\partial\Omega = \Gamma_N \cup \Gamma_D$  and  $\Gamma_N \cap \Gamma_D = \emptyset$ .  $\Gamma_N$  and  $\Gamma_D$  denote the Neumann and Dirichlet boundaries, respectively.  $\delta u$  is the virtual displacement vector from the equilibrium position,  $\nabla^s(\cdot)$  is the symmetric part of the gradient operator used to construct both compatible strain and virtual strain second order tensors,  $\mathbb{D}$  is the linear elastic rigidity tensor of fourth order,  $f$  is the body forces

vector and  $t$  is the vector of prescribed tractions at the static part (Neumann) of the solid's boundary.

The Finite Element Method (FEM), [13], provides a discretization for the weak form of the BVP through a strategy for defining trial/test approximations for the displacement fields involved. At the element level an approximation is constructed by a linear combination of  $n_\alpha$  nodal element shape functions  $\varphi_\alpha^e$  taking as parameters the nodal values  $u_\alpha^e$  of the trial displacement field, as follows:

$$u^e(x) = \sum_{\alpha}^{n_\alpha} \varphi_\alpha^e(x) u_\alpha^e \quad (4)$$

Basically, as shown on what follows, the main difference between the standard FEM and the GFEM is in the definition of the element shape functions.

## 2.1 The GFEM local and global approximations

In short, to comprise the possibility that the solution can change from one part to another of the domain, in the GFEM the approximation is constructed into subdomains called patches. A mesh of finite elements linking  $N$  nodes and discretizing the solid domain is used for defining the nodal patches. The gain of approximation is achieved through augmenting the basic FEM approximation space by exploring the concept of Partition of Unity (PoU) for constructing the local enriched approximations. A variety of PoU can be used, however in the GFEM the PoU is directly supplied by the FEM mesh. Often piecewise linear 'hat' functions provided by the triangular finite element mesh or bilinear functions provided by quadrilateral elements are commonly explored as PoU for two dimensional analysis purposes. One important characteristic of the GFEM is that the underlying mesh keeps unchanged.

As already mentioned before, the shape functions ( $\phi_{\alpha i}$ ) are defined locally in a domain called nodal patch (set of elements having a common node as vertex). Inside of each patch ( $\alpha$ ), the shape functions are constructed by the product between the so-called enrichment functions ( $L_{\alpha i}$ ) and the partition of unity functions belonging to the elements in the patch and attached to the vertex. Therefore, the shape functions for the GFEM are written as:

$$\phi_{\alpha i} = \varphi_\alpha L_{\alpha i} \quad (5)$$

where  $\alpha (=1, \dots, N)$  identifies the nodal patch and  $i (=1, \dots, nl(\alpha))$  identifies the enrichment function ( $nl(\alpha)$  is the total number of enrichment functions adopted for the patch). In the GFEM, normally the first component of the enrichment functions set is assumed as equal to the unity, i.e.  $L_{\alpha 1} = 1$ . Therefore, the FEM approach always belongs to the approximation space of the GFEM.

The enrichment functions can be found from a polynomial basis, if the aim is approximating smooth solutions, or from the available information about the non-smooth solution, if special features are involved in the problem to be considered. However, for the sake of readiness only an enrichment scheme aiming to achieve a certain complete polynomial degree is hereby used.

Accordingly, the general form of the polynomial enrichment component basis can be expressed by the shifted arrangement as

$$L(m,n) = \frac{(X - X_\alpha)^m (Y - Y_\alpha)^n}{h^{m+n}} \quad (6)$$

where  $X_\alpha$  and  $Y_\alpha$  are the coordinates of the patch vertex node  $\alpha$  and  $h$  is a scaling factor given, for instance, by the radius of the circle centered at the vertex and circumscribing the largest element of the patch. One of the most remarkable advantages of the shifted enrichment functions is that they are zero in the node where they are imposed. It follows that the physical meaning of the original degree of freedom associated to the basic part of the approximation at such a node is preserved. Moreover, this feature enables one, in principle, to directly enforce displacement boundary conditions in the same way as in the FEM.

As a rule, in 2-D analysis the enrichment functions are applied to each of the displacement components. Once the enriched approximations are set in each patch a partition of unity is used to paste the local approximations together forming a global regular approximation. Therefore, by restricting only to 2-D problems, the GFEM global approximation for each component of the displacement field is given by the following relations:

$$\hat{u} = \sum_{\alpha=1}^N \varphi_\alpha u_\alpha + \sum_{\alpha=1}^N \sum_{i=2}^{nl} \phi_{\alpha i} b_{\alpha i} \quad (7)$$

$$\hat{v} = \sum_{\alpha=1}^N \varphi_\alpha v_\alpha + \sum_{\alpha=1}^N \sum_{i=2}^{nl} \phi_{\alpha i} c_{\alpha i} \quad (8)$$

where  $u_\alpha$  and  $v_\alpha$  are parameters associated with usual degrees of freedom of the FEM,  $b_{\alpha i}$  and  $c_{\alpha i}$  are additional nodal parameters introduced by enrichment. In the previous relations a convenient splitting of the GFEM approximation space is explored, putting in evidence the basic part provided by the FEM and the enrichment part. Therefore, being  $S_1$  the basic space and  $S_2$  the enrichment space, formally the GFEM approximation space ( $S_{GFEM}$ ) can be represented as follows:

$$S_{GFEM} = S_1 + S_2 \quad (9)$$

$$S_1 = \left\{ \xi : \xi = \sum_{\alpha=1}^N \varphi_\alpha a_{\alpha 1} \right\} \quad (10)$$

$$S_2 = \left\{ \xi : \xi = \sum_{\alpha=1}^N \varphi_\alpha \sum_{i=2}^{nl} L_{\alpha i} a_{\alpha i} \right\}$$

Once trial/test functions given by the approximation space are inserted in the Principle of Virtual Work relation, the resulting discretized weak form provides the specific values for the set of

nodal parameters, therefore associating the finite dimensional global approximation to the exact solution of the BVP.

Of course, the accuracy of the global approximate solution depends on the favorable properties of the local approximation spaces. In this regard, there are no restrictions to the type and number of enrichment functions to be attached to a given node. Therefore, the number of degrees of freedom is totally flexible. Consequently, at the element level, the size of the resulting element stiffness matrix may change drastically, depending on the adopted enrichment scheme. Moreover, once a Galerkin approach is used, the element equivalent forces vectors also present variable sizes.

Notwithstanding the favorable aspects mentioned above, the polynomial enrichment approach may introduce linear dependencies in the resulting system of equations, therefore affecting the numerical stability and accuracy of the method. This kind of issue is well-known as one of the most significant drawbacks of the GFEM. However, as shown in this work, once certain assumptions are satisfied the polynomial enrichment approach can be explored efficiently.

## 2.2 The SGFEM local and global approximations

In the SGFEM the local enrichment functions of the GFEM are modified through a piecewise linear interpolant function, such that the values of the modified enrichment function are zero at all the nodes belonging to the patch.

More precisely, the enrichment functions for a patch ( $\alpha$ ) are constructed by the difference between the original enrichment function ( $L_{\alpha i}$ ) and its piecewise linear or bilinear finite element interpolant function ( $I_{\omega_\alpha}$ ). Therefore,

$$L_{\alpha i}^{\text{mod}} = L_{\alpha i} - I_{\omega_\alpha}(L_{\alpha i}) \quad (11)$$

At the element level the interpolant function can be written as:

$$I_{\omega_\alpha} = \sum_{j=1}^{n_\alpha} \varphi_j L_{\alpha i}(X_j, Y_j) \quad (12)$$

where  $(X_j, Y_j)$  are the coordinates of node  $j$  of the element in question.

The identical procedure for constructing the GFEM shape functions is then used to define the SGFEM shape functions ( $\phi_{\alpha i}^{\text{mod}}$ ). Hence,

$$\phi_{\alpha i}^{\text{mod}} = \varphi_\alpha L_{\alpha i}^{\text{mod}} \quad (13)$$

Thus, it is convenient to represent the SGFEM approximation space as follows:

$$S_{SGFEM} = S_1 + S_2^{\text{mod}} \quad (14)$$

$$S_1 = \left\{ \xi : \xi = \sum_{\alpha=1}^N \varphi_{\alpha} a_{\alpha 1} \right\} \quad (15)$$

$$S_2^{\text{mod}} = \left\{ \xi : \xi = \sum_{\alpha=1}^N \varphi_{\alpha} \sum_{i=2}^{nl(\alpha)} L_{\alpha i}^{\text{mod}} a_{\alpha i} \right\}$$

The interpolant function and the resulting shape function considered in SGFEM are highlighted in Figure 1.

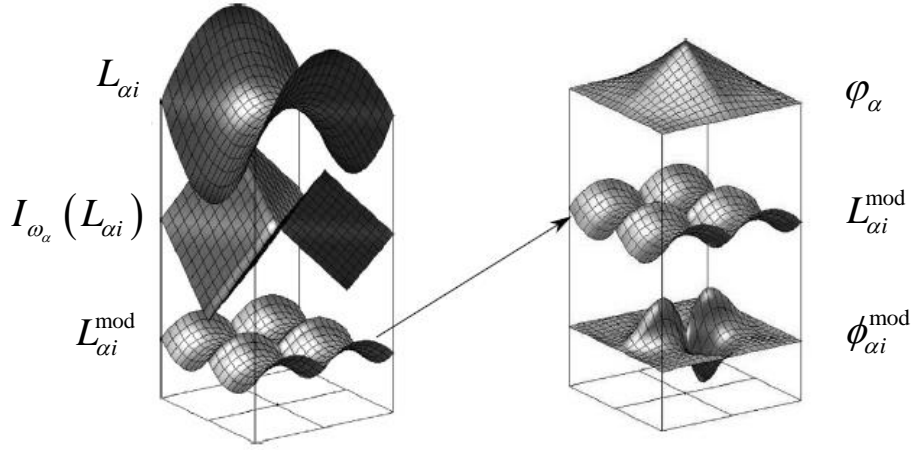


Figure 1: Construction of an enrichment function and a shape function used in SGFEM, adapted from Figure 2 of [16].

It can be shown, [11], that the SGFEM retains the good approximation property of the GFEM. Moreover, as the mesh refinement increases, the conditioning of the SGFEM is asymptotically not worse than that of the conventional Finite Element Method. However, those good features require satisfaction of the linear independence among the enriched shape functions. Such an aspect is addressed next.

### 3 THE HIGHER ORDER SGFEM

The higher order SGFEM yields higher order convergence and presents good conditioning derived from a further specific modification of the enrichment space, which is simple enough for retaining the good flexibility for constructing local enriched approximations as in the standard SGFEM.

Such an additional modification aims to guarantee that the shape functions of the enriched space be locally linearly independent. Essentially, the procedure hereby adopted consists of using another PoU for constructing the  $S_2^{\text{mod}}$  space, different from the piecewise hat functions that

however are preserved for constructing the basic  $S_l$  space. Thus, the higher order SGFEM approximation space is represented as follows:

$$S_{SGFEM} = S_1 + S_2^{\text{mod}} \quad (16)$$

$$S_1 = \left\{ \xi : \xi = \sum_{\alpha=1}^N \varphi_{\alpha} a_{\alpha 1} \right\} \quad (17)$$

$$S_2^{\text{mod}} = \left\{ \xi : \xi = \sum_{\alpha=1}^N N_{\alpha} \sum_{i=2}^{nl(\alpha)} L_{\alpha i}^{\text{mod}} a_{\alpha i} \right\}$$

In the  $S_2^{\text{mod}}$  space definition,  $L_{\alpha i}^{\text{mod}}$  is constructed just as indicated in relation (11), while  $N_{\alpha}$  represents the so called ‘flat-top’ function, [14], hereby adopted as PoU.

The ‘flat-top’ function can be constructed element-wise. In 1-D it can be easily defined by considering a unitary domain,  $\Omega = (0,1)$  discretized by  $N$  nodes equally spaced. If  $h$  is the distance between a pair of nodes, then the nodal coordinates are given by:  $\{x_i = ih\}_{i=0}^N$ . For a parameter  $0 \leq \sigma < 0.5$  and a positive integer  $l$ , the element-wise flat-top PoU is defined as follows:

$$N_{Left}^{\sigma}(x) = \begin{cases} 1 & x \in [x_j, x_j + \sigma h] \\ \left( 1 - \left( \frac{x - x_j - \sigma h}{(1 - 2\sigma)h} \right)^l \right)^l & x \in [x_j + \sigma h, x_j + (1 - \sigma)h] \\ 0 & x \in [x_j + (1 - \sigma)h, x_{j+1}] \end{cases} \quad (18)$$

$$N_{Right}^{\sigma}(x) = \begin{cases} 0 & x \in [x_j, x_j + \sigma h] \\ 1 - \left( 1 - \left( \frac{x - x_j - \sigma h}{(1 - 2\sigma)h} \right)^l \right)^l & x \in [x_j + \sigma h, x_j + (1 - \sigma)h] \\ 1 & x \in [x_j + (1 - \sigma)h, x_{j+1}] \end{cases} \quad (19)$$

In the relations above,  $x$  is a local coordinate with origin at the left node of the element ( $x_j$ ),  $N_{Left}^{\sigma}(x)$  is for the PoU component attached to the node  $x_j$  and  $N_{Right}^{\sigma}(x)$  is the PoU component attached to node  $x_{j+1}$ .

In 2-D the flat-top can be constructed on the master element trough the tensorial product between the 1-D components above indicated. The flat-top functions for 1-D and 2-D quadrilateral master element hereby considered in the higher order SGFEM are represented in Figure 2. The cases depicted correspond to  $\sigma = 0.25$  and  $l = 1$ .

$$N_{Left}^{\sigma}(x) \quad N_{Right}^{\sigma}(x)$$

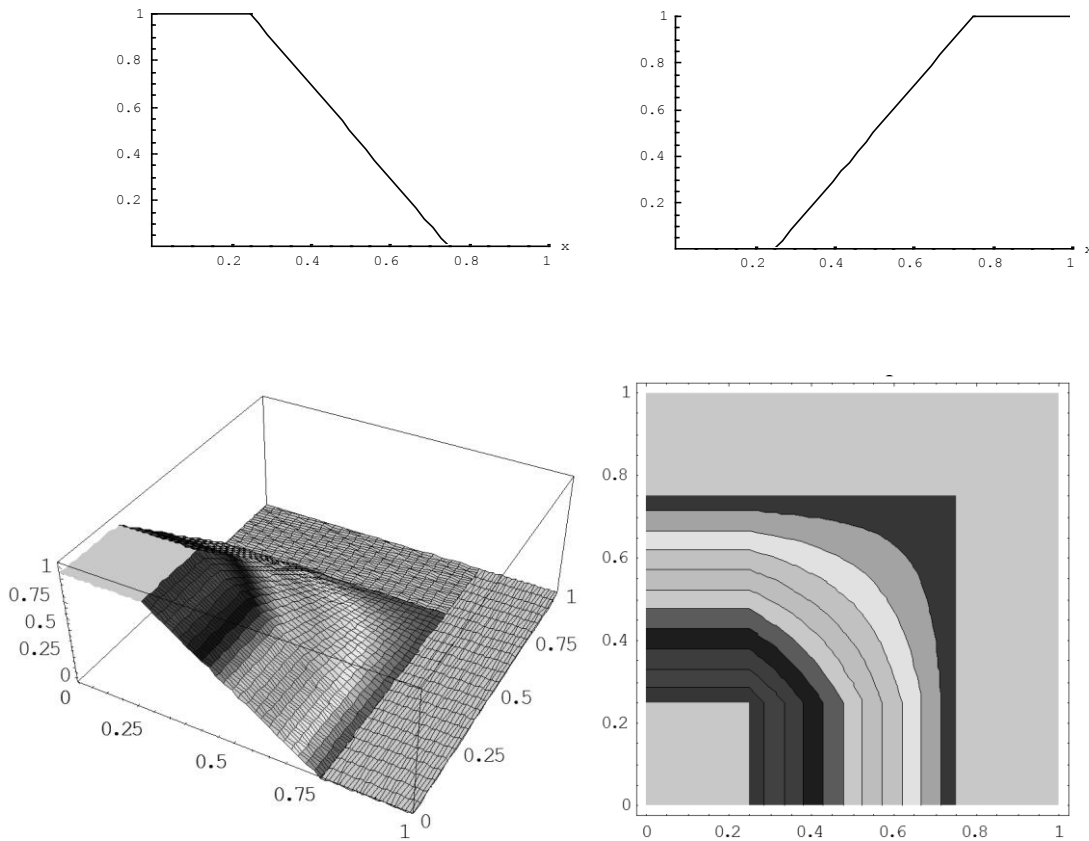


Figure 2: Flat-top partition of unity, 1-D and 2-D illustrations

To deal with the numerical integration of the stiffness matrix components as well of the equivalent nodal forces vector with flat-top functions, an appropriate strategy is conceived. Therefore, subdomains are attributed to the element in agreement with the piecewise definition of the 'flat-top' function inside the element, and standard quadrature rules applied in each subdomain. The implementations were done using a Python based computational code for the GFEM following the object-oriented programming paradigm, described in [15].

#### 4 NUMERICAL EXAMPLES

In what follows, two numerical examples are presented. In each of them, only structured meshes and enrichment schemes with shifted polynomial functions were investigated.

The first example is related to an L-shaped domain aiming essentially to evaluate accuracy of displacement and stress results that can be provided by the higher order SGFEM. Convergence

order and scaled condition number are presented by confronting the results of the standard GFEM and SGFEM.

The second example aims to illustrate the potential of the higher order SGFEM even if a crack is included at one edge of a panel. Again, the accuracy and stability of the method are shown through the analysis of the convergence order and scaled condition number.

Despite of local non-smoothness implicit in both examples, it is shown that the method provides asymptotic convergence with mesh refinement.

#### 4.1 L-shaped panel

The first example consists of an L-shaped panel under uniform distributed loading at the longer edges, as depicted in Figure 3. Sliding supports are prescribed at the Dirichlet's boundaries. The material has a linear elastic response, being adopted Young's modulus of 100 and Poisson's ratio of 0.3 as elastic parameters. Moreover, unitary thickness and plane stress conditions are assumed.

Six structured meshes varying from coarse to fine and composed by bilinear quadrilateral elements are used in this case. These meshes present the following grid sizes, indicated according to the number of elements in the longer and shorter edges, respectively as: 4 x 2, 8 x 4, 16 x 8, 32 x 16, 64 x 32 and 128 x 64.

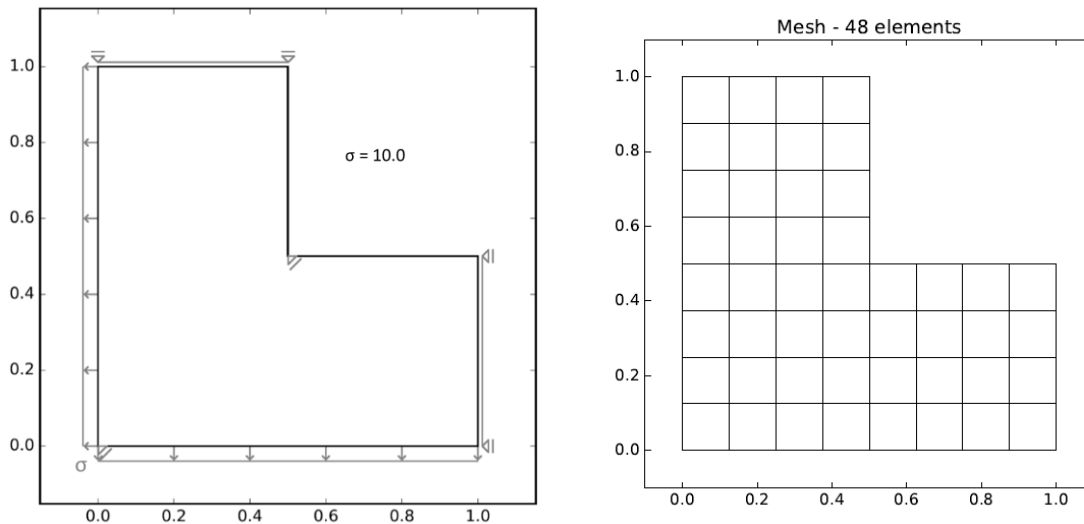


Figure 3: L-shaped panel

Shifted complete and incomplete second degree polynomial options of enrichment are considered and applied to the whole set of nodes. Accordingly, the complete case is configured by adopting in relation (6) the set of parameters:  $(m = 2; n = 0)$ ,  $(m = 0; n = 2)$ ,  $(m = 1; n = 1)$ . The incomplete case takes only the first two sets of parameters, corresponding to the quadratic terms. Furthermore, Dirichlet's boundary conditions were imposed through penalization technique.

In this situation, a comparison between GFEM, SGFEM and higher order SGFEM is presented. The main aspects evaluated are rate of convergence based on the estimate errors on displacements and scaled condition number.

The relative error on displacements is computed using the  $L_2$  norm as follows:

$$relative\ error = \frac{\|u_{ref} - \tilde{u}\|_{L_2}}{\|u_{ref}\|_{L_2}} \quad (20)$$

In the relation above,  $u_{ref}$  is for the reference solution computed by FEM using a very refined mesh (2048 x 1024) and  $\tilde{u}$  is for the approximate solution. The relative errors for the case of incomplete enrichment are reported in Table 1.

Table 1 Relative errors

Mesh h	$h^{-1}$	FEM	SGFEM	FT sig = 0.25
4	0,25	0,1423	0,062667	0,090534
8	0,125	0,067426	0,028571	0,039220
16	0,0625	0,030463	0,013264	0,017848
32	0,03125	0,013698	0,006088	0,008191
64	0,015625	0,006147	0,002719	0,003699
128	0,0078125	0,002706	0,001139	0,001597

The h-convergence of the relative errors for the case of incomplete enrichment is shown by the log-log graphs depicted in Figure 4. This is not a regular problem as the reentrant corner induces stress singularity. Even so, it can be observed that comparing SGFEM and SGFEM/Flat-Top PoU with FEM the convergence rates are pretty much of the same order.

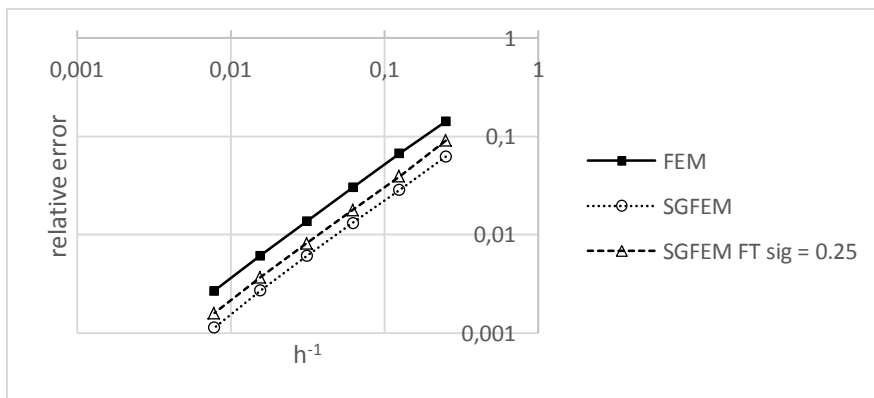


Figure 4: L-shaped panel – Relative error values with respect to mesh refinement

Another important measure to compare is the scaled condition number (SCN). Following [11], this value is given by the ratio between the highest and the lower eigenvalues of the scaled stiffness matrix of the linear system associated to the SGFEM. Representing by  $K$  the stiffness matrix, the scaled one is defined as:

$$\hat{K} = DKD \quad (21)$$

where  $D$  is a diagonal matrix in which the diagonal terms are computed as:  $D_{ii} = K_{ii}^{-1/2}$ .

In Figure 5 the SCN is compared for the incomplete enrichment case. It can be seen that the values obtained from SGFEM and higher order SGFEM are close to the values provided by FEM analysis. Actually, the flat-top option does not present any advantage with respect to the SGFEM, once the incomplete enrichment space verifies the orthogonality condition.

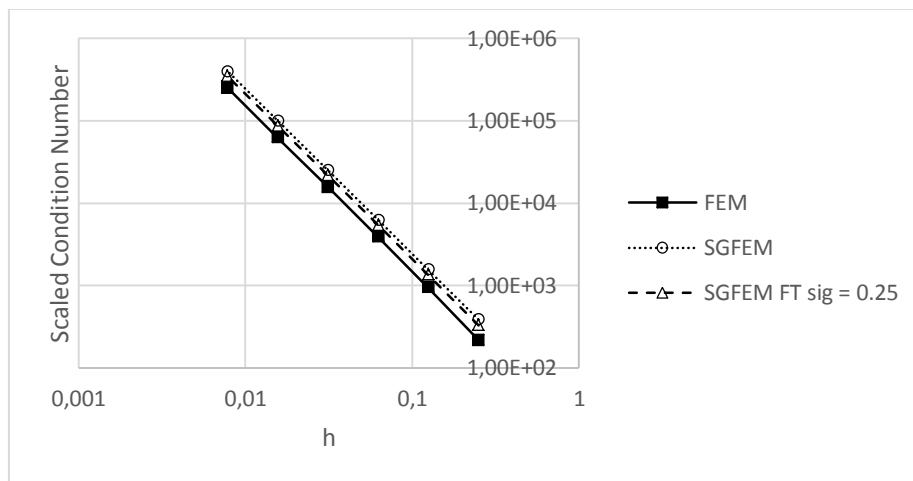


Figure 5: L-shaped panel – Scaled condition number with respect to mesh refinement

However, when a complete enrichment is considered, the SCN is strongly affected in the SGFEM, which remains comparable to the bad condition level shown by GFEM, as reported in Table 2. This is evidence that the resulting enriched space lacks of orthogonality. However, orthogonality is preserved when using Flat-Top PoU for the enrichment space, being such advantage marked by the corresponding SCN drop to values of the order of FEM.

Table 2 Scaled Condition Number

Mesh h	$h^{-1}$	FEM	GFEM	SGFEM	FT sig = 0.25
4	0,25	2,16E+02	1,18E+19	1,89E+19	3,39E+02
8	0,125	9,43E+02	1,19E+18	1,95E+17	1,40E+03
16	0,0625	3,87E+03	1,33E+19	1,09E+19	5,23E+03
32	0,03125	1,56E+04	1,71E+18	4,20E+18	2,09E+04

Finally, the SGFEM using Flat-Top PoU benefits from the mesh refinement, as shown in Figure 6.

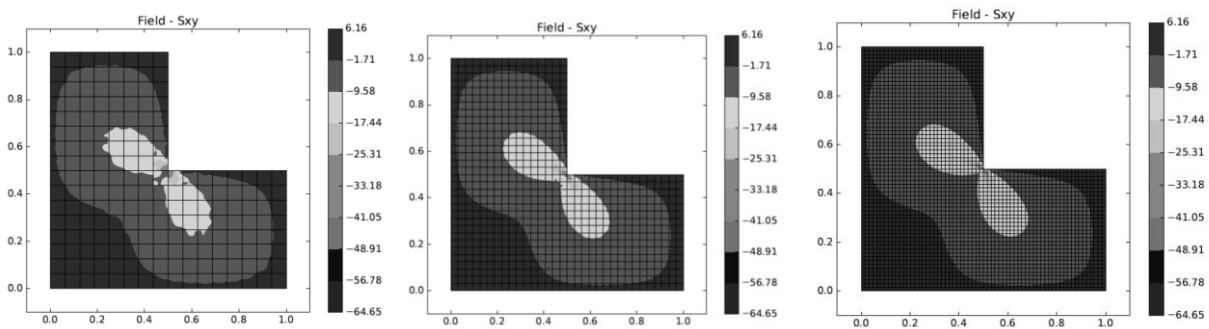


Figure 6: Effect of mesh refinement (16X8), (32X16), (64X32)

## 4.2 Panel presenting an edge crack

The selected problem for analysis is presented in Figure 7.

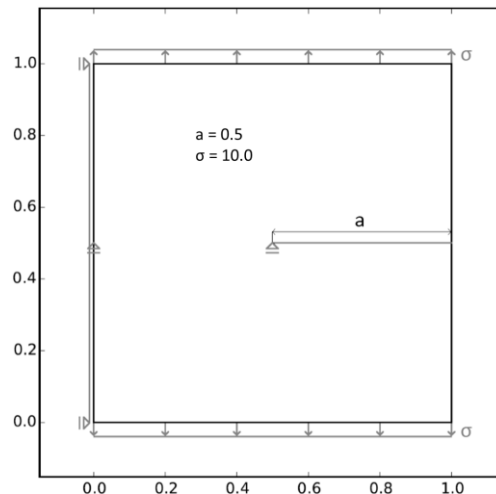


Figure 7: Edge cracked panel

Sliding supports are prescribed at the Dirichlet's boundaries and uniformly distributed loading on the top and bottom edges. The material has a linear elastic response, being adopted Young's Modulus of 100 and Poisson's ratio of 0.3 as elastic parameters. Moreover, unitary thickness and plane stress conditions are assumed.

Six structured meshes varying from coarse to fine and composed by bilinear quadrilateral elements are used in this case. These meshes present the following grid sizes, indicated according to the number of elements in the horizontal and vertical directions, respectively as: 4 x 4, 8 x 8, 16 x 16, 32 x 32, 64 x 64 and 128 x 128.

Analogous to the previous example, shifted complete and incomplete second degree polynomial options of enrichment are considered and applied to the whole set of nodes. Again, a comparison between GFEM, SGFEM and higher order SGFEM is presented. The main aspects evaluated are rate of convergence based on the estimate errors on displacements and scaled condition number.

In the relation above,  $u_{ref}$  is for the reference solution computed by FEM using a very refined mesh (2048 x 2048) and  $\hat{u}$  is for the approximate solution. The relative errors on displacements computed using the  $L_2$  norm for the case of incomplete enrichment are reported in Table 3.

Table 3 Relative errors

Mesh h	$h^{-1}$	FEM	SGFEM	FT sig = 0.25
4	0,25	0,216344	0,151842	0,185781
8	0,125	0,14344	0,082748	0,098132
16	0,0625	0,074208	0,043917	0,051456
32	0,03125	0,037411	0,02247	0,026295
64	0,015625	0,018531	0,011134	0,013072
128	0,007813	0,008976	0,005299	0,006276

The h-convergence of the relative errors for the case of incomplete enrichment is shown by the log-log graphs depicted in Figure 8. This is not a regular problem as the crack induces heavy stress singularity. Even so, it can be observed that comparing SGFEM and SGFEM/Flat-Top PoU with FEM the convergence rates are pretty much of the same order.

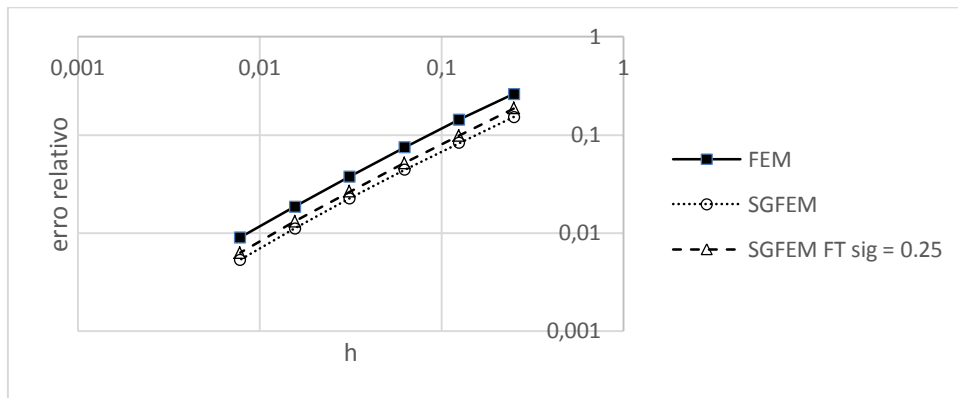


Figure 8: Edge cracked panel – Relative error values with respect to mesh refinement

In Figure 9 the scaled condition number (SCN) is compared for the incomplete enrichment case. It can be seen that the values obtained from SGFEM and higher order SGFEM are close to the values provided by FEM analysis. Actually, the flat-top option does not present any advantage with respect to the SGFEM, once the incomplete enrichment space verifies the orthogonality condition.

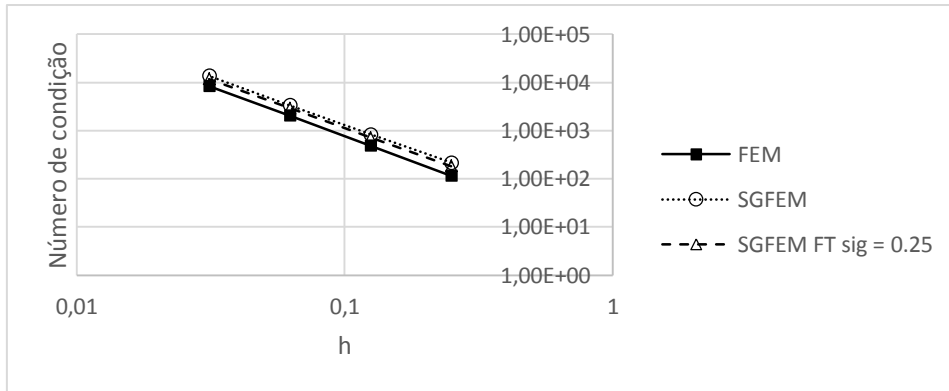


Figure 9: Edge cracked panel – Scaled condition number with respect to mesh refinement

However, when a complete enrichment is considered, the SCN is strongly affected in the SGFEM, which remains comparable to the bad condition level shown by GFEM, as reported in Table 4. This is evidence that the resulting enriched space lacks of orthogonality. However, orthogonality is preserved when using Flat-Top PoU for the enrichment space, being such advantage marked by the corresponding SCN drop to values of the order of FEM.

Table 4 Scaled Condition Number

Mesh h	$h^{-1}$	FEM	GFEM	SGFEM	FT sig = 0.25
4	0,25	1,16E+02	3,89E+15	9,75E+14	1,84E+02
8	0,125	4,89E+02	6,67E+14	3,37E+14	7,21E+02
16	0,0625	2,05E+03	1,81E+15	3,59E+14	2,92E+03
32	0,03125	8,42E+03	1,41E+18	5,48E+15	1,19E+04

Finally, the SGFEM using Flat-Top PoU benefits from the mesh refinement, as shown in Figure 10.

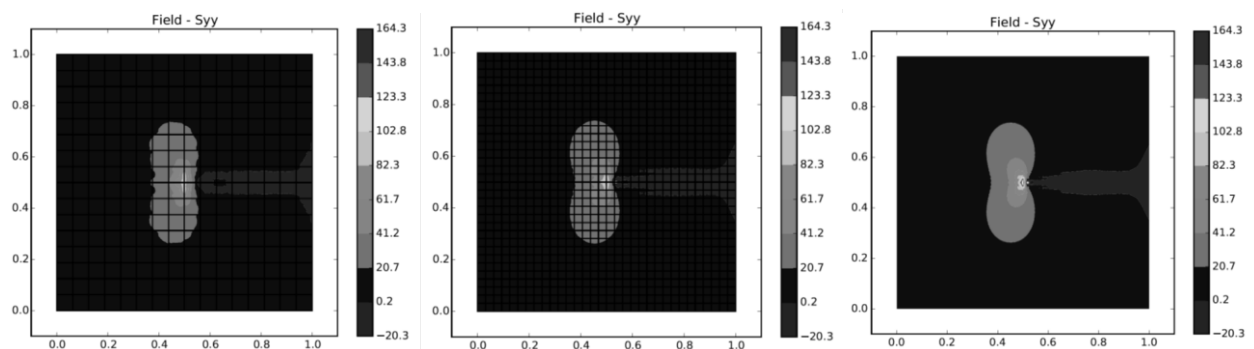


Figure 10: Effect of mesh refinement (16X16), (32X32), (64X64)

## 5 CONCLUSION

The numerical investigation carried on the SGFEM comprised the use of a flat-top partition of unity for modifying the enriched approximation space. Shifted polynomial functions were considered for the enrichment of the partition of unity. As polynomial enrichments can introduce linear dependencies, affecting numerical stability, the main purpose of this investigation was to give a contribution by further investigating the SGFEM stability through modifying the enrichment and computing the condition number of the resulting system of equations.

It was shown that the scheme chosen for constructing the approximation space yields scaled condition numbers of the same order as the one provided by the conventional finite element method, therefore minimizing discretization errors. Moreover, the resulting orders of convergence are comparable to the ones exhibited by the GFEM, therefore, indicating favorably towards the numerical accuracy.

## 6 ACKNOWLEDGEMENTS

The authors would like to thank CAPES (Coordination for the Improvement of Higher Education Personnel) and FAPESP (São Paulo Research Foundation) for the financial support.

## REFERENCES

- [1] Melenk, J. M. and Babuška, I., 1996. "The partition of unity finite element method: basic theory and applications". *Computer Methods in Applied Mechanics and Engineering*, vol. 39, pp.289-314.
- [2] Belytschko, T., Gracie, R. and Ventura, G., 2009. "A review of the extended/generalized finite element methods for material modelling". *Modelling and Simulation in Materials Science and Engineering*, vol.17, 24 pp.
- [3] Belytschko, T. and Black, T., 1999. "Elastic crack growth in finite elements with minimal remeshing". *International Journal for Numerical Methods in Engineering*, vol. 45, pp. 601-620.
- [4] Moës, N., Dolbow, J. and Belytschko, T., 1999. "A finite element method for crack growth without remeshing". *International Journal for Numerical Methods in Engineering*, vol. 46, pp.131-150.
- [5] Duarte, C.A., Hamzeh, O.N., Lyszka, T.J. and Tworzydło, W.W., 2001. "A generalized finite element method for the simulation of three-dimensional dynamic crack propagation". *Computer Methods in Applied Mechanics and Engineering*, vol. 15, pp.2227-2262.
- [6] Pereira, J.P., Duarte, C.A., Guoy, D. and Jiao, X., 2009. "HP-Generalized FEM and crack surface representation for non-planar 3-D cracks". *International Journal for Numerical Methods in Engineering*, vol. 77, pp.601-633.
- [7] Sukumar, N., Moës, B., Moran, B. and Belytschko, T., 2000. "Extended finite element method for three-dimensional crack modelling". *International Journal for Numerical Methods in Engineering*, vol. 48, pp.1549-1570.

- [8] Sukumar, N., Srolovitz, D.J., Baker, T.J. and Prévost, J.H., 2003. "Brittle fracture in polycrystalline microstructures with the extended finite element method". *International Journal for Numerical Methods in Engineering*, vol. 56, pp.2015-2037.
- [9] Simone, A., Duarte, C.A. and van der Griessen, E., 2006. "A generalized finite element method for polycrystals with discontinuous grain boundaries". *International Journal for Numerical Methods in Engineering*, vol. 67, pp.1122-1145.
- [10] Alfaiate, J., Simone, A. and Sluys, L.J., 2003. "Non-homogeneous displacement jumps in strong embedded discontinuities". *International Journal for Numerical Methods in Engineering*, vol. 40, pp.5799-5817.
- [11] Babuška I. and Banerjee U., 2011. "Stable generalized finite element method (SGFEM)". *Computer Methods in Applied Mechanics and Engineering*, 201-204, pp.91-111.
- [12] Zhang, Q., Banerjee U. and Babuška I., 2014. "Higher order stable generalized finite element method". *Numerische Mathematik*, 128: 1. doi: 10.1007/s00211-014-0609-1.
- [13] Hughes, T.J.R., 2000. *The Finite Element Method: Linear Static and Dynamic Finite Element Analysis*, Prentice-Hall, Inc, New Jersey.
- [14] Griebel, M. and Schweitzer, M.A., 2002. "A particle-partition of unity method, Part II: efficient cover construction and reliable integration". *SIAM J. Sci. Comput.* 23(5), 1655-1682.
- [15] Piedade Neto, D., Ferreira, M.D.C. and Proença, S.P.B., 2013. "An Object-Oriented class design for the Generalized Finite Element Method programming". *Latin American Journal of Solids and Structures*, vol.10, pp.1267-1291.
- [16] Gupta V., Duarte C.A., Babuška I. and Banerjee, U. 2013. "A stable and optimally convergent generalized FEM (SGFEM) for linear elastic fracture mechanics". *Comput. Methods Appl. Mech. Eng.*, 266:23-39.

## **RESPONSIBILITY NOTICE**

The authors are the only responsible for the printed material included in this paper.